Nucleocytoplasmic shuttling of soluble tubulin in mammalian cells

Tonia Akoumianaki[1], Dimitris Kardassis[1,2], Hara Polioudaki[1], Spyros D. Georgatos[3,4] and Panayiotis A. Theodoropoulos[1,*]

[1]Department of Biochemistry, University of Crete, School of Medicine, 71 003 Heraklion, Greece
[2]Institute of Molecular Biology and Biotechnology, Foundation for Research and Technology-Hellas, 71 110 Heraklion, Greece
[3]Stem Cell and Chromatin Group, The Laboratory of Biology, University of Ioannina School of Medicine, 45 110 Ioannina, Greece
[4]The Biomedical Institute of Ioannina, IBE/ITE, 45 110 Ioannina, Greece
*Author for correspondence (e-mail: takis@med.uoc.gr)

Accepted 17 December 2008
Journal of Cell Science 122, 1111-1118 Published by The Company of Biologists 2009
doi:10.1242/jcs.043034

Summary

We have investigated the subcellular distribution and dynamics of soluble tubulin in unperturbed and transfected HeLa cells. Under normal culture conditions, endogenous α/β tubulin is confined to the cytoplasm. However, when the soluble pool of subunits is elevated by combined cold-nocodazole treatment and when constitutive nuclear export is inhibited by leptomycin B, tubulin accumulates in the cell nucleus. Transfection assays and FRAP experiments reveal that GFP-tagged β-tubulin shuttles between the cytoplasm and the cell nucleus. Nuclear import seems to occur by passive diffusion, whereas exit from the nucleus appears to rely on nuclear export signals (NESs). Several such motifs can be identified by sequence criteria along the β-tubulin molecule and mutations in one of these (NES-1) cause a significant accumulation in the nuclear compartment. Under these conditions, the cells are arrested in the G0-G1 phase and eventually die, suggesting that soluble tubulin interferes with important nuclear functions. Consistent with this interpretation, soluble tubulin exhibits stoichiometric binding to recombinant, normally modified and hyper-phosphorylated/acetylated histone H3. Tubulin-bound H3 no longer interacts with heterochromatin protein 1 and lamin B receptor, which are known to form a ternary complex under in vitro conditions. Based on these observations, we suggest that nuclear accumulation of soluble tubulin is part of an intrinsic defense mechanism, which tends to limit cell proliferation under pathological conditions. This readily explains why nuclear tubulin has been detected so far only in cancer or in transformed cells, and why accumulation of this protein in the nucleus increases after treatment with chemotherapeutic agents.

Supplementary material available online at
http://jcs.biologists.org/cgi/content/full/122/8/1111/DC1

Key words: Nuclear export, Tubulin, Histones, β-tubulin, Subcellular distribution

Introduction

The eukaryotic genome encodes several tubulin proteins, which belong to six distinct families: α-, β-, γ-, δ-, ε- and ζ-tubulin (McKean et al., 2001). Dimeric α/β-tubulin is the building block of microtubules and is encoded by multiple genes (Luduena, 1998). Thus, mammals appear to have six forms of α and seven forms of β tubulin that differ in their C-terminal or N-terminal regions, and further categorized in distinct sub-classes (Sullivan, 1988). The relative composition of α- and β-tubulin isoforms affects the structure and function of microtubules (Lu and Luduena, 1994; Rezania et al., 2008). Tubulin mutations and various post-translational modifications, such as acetylation, palmitoylation, phosphorylation, polyglutamylation, polyglycylation and detyrosination also affect microtubule structure under a variety of normal or pathological conditions (Burkhart et al., 2001; Luduena, 1998; McKean et al., 2001; Sullivan, 1988).

Although soluble α/β-tubulin is considered to be a reservoir of subunits that are available for microtubule polymerization in the cytoplasm, there are several reports supporting the presence of tubulin in the nucleus of cultured animal cells (Goo et al., 2003; Menko and Tan, 1980; Walss-Bass et al., 2002; Xu and Luduena, 2002). Nuclear tubulin is thought to associate with chromatin (Menko and Tan, 1980) and interact in vitro with core and linker histones (Mithieux et al., 1984).

Earlier immunocytochemical studies have indicated that βII-tubulin is the main nuclear isoform (Walss-Bass et al., 2002; Xu and Luduena, 2002). This subtype has been suggested to modulate Notch signaling, via binding to the Notch1 receptor and C promoter-binding factor 1 response elements (Yeh et al., 2004). Furthermore, human α3 and β1 tubulin have been identified in a nuclear complex containing, among other proteins, the nucleolar constituent fibrillarin (Yanagida et al., 2004). It has been speculated that these tubulin forms are involved in the transport of fibrillarin-associated subcomplexes to different nuclear compartments, including the nucleolus and the Cajal bodies.

Using polyclonal antibodies, α/β-tubulin has been detected in the nucleus of MCF-7 cells and found to co-precipitate with ASC-2, a transcriptional co-activator amplified in human cancers and capable of stimulating trans-activation by numerous nuclear receptors and transcription factors (Goo et al., 2003). Moreover, α/β-tubulin dimers co-purify with ASC-2, the Trithorax group proteins HALR and ASH2, and the retinoblastoma-binding protein RBQ-3, as an ~2 MDa complex (ASC-2 complex) (Goo et al., 2003).

Ectopically localized microtubules and α-tubulin have been detected in subpopulations of cisplatin-treated C6 glioma astrocytes

(Krajci et al., 2006), whereas acetylated α-tubulin has been found in intra-nuclear inclusions of neuroblastoma N2a cells overexpressing collapsing response mediator protein 2 (Gu and Ihara, 2000). In HeLa cells, β-tubulin has been shown to colocalize with co-factor D (Martin et al., 2000), whereas, in plants, native and GFP-tagged α-tubulin have been found to accumulate reversibly in the nuclei of cultured tobacco cells in response to low temperature (Schwarzerova et al., 2006). Finally, in the fungus *A. nidulans*, tubulin levels in the nucleoplasm are differentially regulated during interphase and mitosis (Ovechkina et al., 2003).

Taking into account all these observations, we decided to study the subcellular distribution and dynamics of soluble tubulin in unperturbed and transiently transfected HeLa cells. We have found that β-tubulin shuttles between the cytoplasm and the cell nucleus, associating specifically with components of chromatin. The functional significance of these findings and the specific mechanisms involved in the transport process are described below.

Results

Endogenous soluble tubulin accumulates in HeLa cell nuclei

Initiating this study, we compared the subcellular distribution of endogenous α/β-tubulin under normal conditions and under conditions that promote microtubule depolymerization, using immunofluorescence microscopy. When HeLa cells were incubated in the presence of nocodazole at 4°C, α- and β-tubulin accumulated in the nucleus of most of the cells (82%) (see Fig. 1A, upper panels). However, nuclear tubulin exited the cell nucleus immediately after the cells were transferred to normal medium and cultured at 37°C (Fig. 1A, lower panel), indicating nucleo-cytoplasmic shuttling that probably involves diffusion-driven import and active nuclear export.

To examine whether the nuclear export of endogenous soluble tubulin depends on previously identified export machinery (e.g. exportin 1), HeLa cells that had been pre-treated with nocodazole at 4°C were transferred to 37°C and cultured in the presence or absence of leptomycin B (LMB). As shown in Fig. 1B, no cells exhibiting nuclear staining could be identified in the control, but tubulin was retained in the nucleoplasm of LMB-treated cells. These results suggested an involvement of exportin 1 in the regulated export of soluble tubulin.

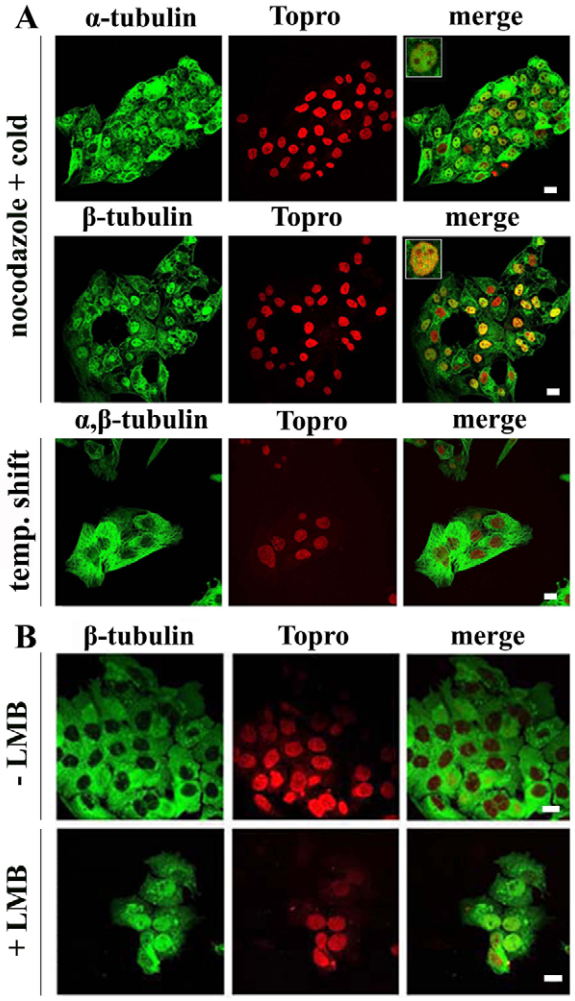

Fig. 1. Reversible accumulation of endogenous tubulin in the nuclei of HeLa cells is inhibited by LMB. (A) Distribution of endogenous α/β-tubulin in HeLa cells under microtubule depolymerization conditions (nocodazole+cold) and after a temperature shift to normal temperature (temp. shift). (B) Effect of leptomycin B (LMB) on nuclear export of endogenous tubulin (for details see Materials and Methods). Cells were fixed and stained with anti-tubulin antibodies immediately after treatment as described in Materials and Methods. DNA was stained with Topro. Scale bars: 20 μm.

Overexpressed GFP-βII/βIV-tubulin partition with both the cytoplasm and the nucleus

We next sought to investigate the subcellular distribution of soluble tubulin using two GFP-tagged isoforms, βII- and βIV-tubulin, transiently expressed in HeLa cells. To examine whether the presence of the GFP moiety affects β-tubulin localization, we examined the behavior of the fusion proteins during mitosis. Both GFP-βIV-tubulin and GFP-βII-tubulin were efficiently incorporated into the spindle microtubules and partitioned, from early prophase to telophase, similarly to endogenous tubulin (Fig. 2 and data not shown).

In view of this, we then examined the localization pattern of GFP-tagged βII/βIV-tubulin in interphase cells. In addition to cytoplasmic staining, β-tubulin subunits accumulated, albeit at a different level, in the nucleus of transfected HeLa cells. Nuclear β-tubulin was uniformly distributed throughout the nucleoplasm, but was almost completely excluded from nucleoli (Fig. 3A). To quantify the levels of nuclear GFP-βII- and GFP-βIV-tubulin in transfected HeLa cells, we measured the fluorescence intensity in both the cytoplasm and in the nucleus (Fig. 3B). Interestingly, when the ratio of nuclear/cytoplasmic staining of βII- and βIV-tubulin was assessed as a function of time (Fig. 3C), each β-tubulin subtype exhibited a distinct temporal pattern. For example, nuclear accumulation of GFP-βIV-tubulin peaked 6 hours post-transfection and steadily declined thereafter reaching a minimum at 72 hours. On the other hand, nuclear accumulation of GFP-βII-tubulin was relatively delayed, peaking 24 hours post-transfection and declining with a lower rate. These data indicate that nuclear translocation of β-tubulin is a dynamic process and depends on tubulin subtype.

Dynamics of β-tubulin in transfected cells

To assess more precisely β-tubulin dynamics, we expressed GFP–βII/βIV-tubulin in HeLa cells and performed FRAP experiments. Quantitative data summarized in Table 1 show that both tubulin subtypes were exceedingly mobile, exhibiting almost complete (~95%) recovery in less than 2 minutes. Nonetheless, cytoplasmic β-tubulin was significantly less mobile than nuclear, with recovery half-times differing almost by a factor of 2. The rapid

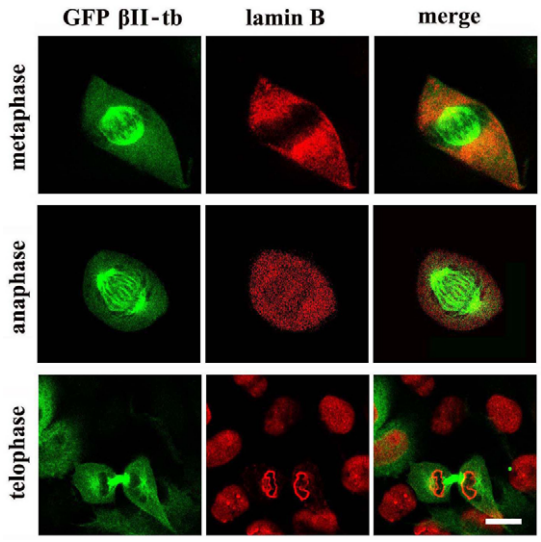

Fig. 2. Distribution of GFP-tagged β-tubulin during mitosis. HeLa cells transiently transfected with GFP-tagged βII-tubulin, cultured for 24 hours and immunostained for lamin B. Representative confocal images from metaphase to telophase are depicted. Scale bar: 20 μm.

kinetics and the differences detected between the cytoplasmic and the nuclear pool were not due to photodamage and cleavage of the β-tubulin moiety from the fusion protein in the different compartments: when analogous experiments were carried out using GFP (monomeric) or RFP (oligomeric) alone, the fluorescence recovery half-times in the nucleus were significantly lower than that of the fusion proteins. Taken together, these results suggest that nuclear βII- and βIV-tubulin are probably in a soluble, yet transiently bound, form.

Nuclear export of GFP-β-tubulin is mediated by distinct NES sequences

Inspecting the sequences of βII- and βIV-tubulin, we could not identify consensus nuclear localization signals (NLSs), consistent with the idea that soluble tubulin is imported into the nucleus by passive diffusion. However, when we searched for nuclear export signals (NESs) bearing homology to the consensus motif Z-$X_{(1-4)}$-J-$X_{(2-3)}$-Z-X-Z [where Z corresponds to L, I or V; J corresponds to M or F; and X corresponds to any amino acid (Mirski et al., 2003)], we could readily detect five such stretches (NES 1-5). Four of these motifs (NES 2-5) were located in the middle part of the polypeptide chain and one (NES-1) at the N-terminal end (Fig. 4A).

To find out whether nuclear export of tubulin is mediated by these putative NESs, we constructed two forms of mutated βII-tubulin, in which Leu residues of NES-1 or NES-2 were replaced by Ala (disNES-1 and disNES-2) (Fig. 4A). The choice of NES-1 and NES-2 was based on structural data (Lowe et al., 2001; Nogales et al., 1998), indicating that these regions, in contrast to NES-3, NES-4 and NES-5, are located in surface-exposed loops and therefore constitute potential sites for exportin 1 binding (Fig. 4B).

When wild-type and mutant β-tubulin were transiently expressed in HeLa cells for 3, 24 and 48 hours, we observed a significant increase in the nuclear accumulation of disNES-1, but not of disNES-2 (Fig. 4C). The median values of the nuclear/cytoplasmic ratios ranged from 0.43-0.49 for wild type, 1.07-1.31 for disNES-1 and 0.55-0.59 for disNES-2. And, furthermore, unlike the cells that were transfected with disNES-2 or wild-type βII-tubulin, 59-

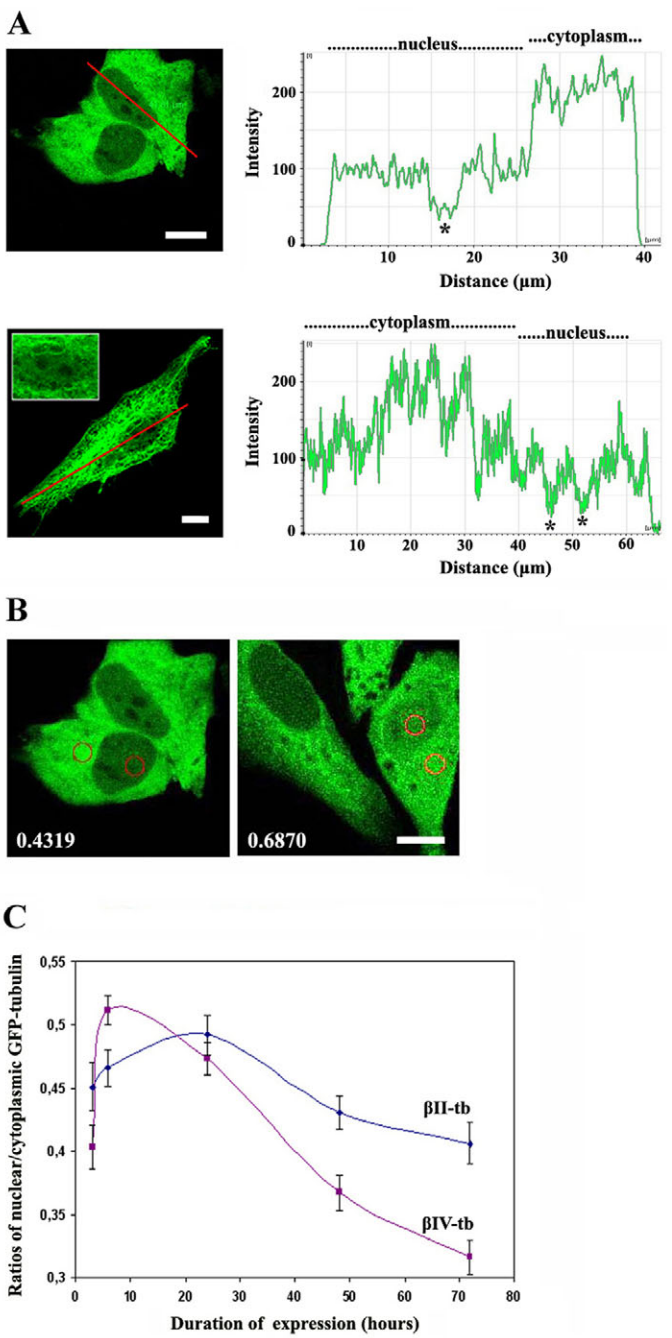

Fig. 3. Distribution of GFP-tagged β-tubulin in interphase HeLa cells. Cells transiently transfected with GFP-tagged β-tubulin were fixed and surveyed by confocal microscopy. (A) Distribution of βII-tubulin in untreated (upper panel) and Triton-X extracted (lower panel) cells. The linescans on the right depict distance versus fluorescence intensity profiles calculated using the LCS Lite Leica software. Asterisks denote the presence of nucleoli. Note the almost uniform distribution of fluorescence in both the cytoplasm and the nucleus, with the exception of the nucleolus in untreated cells and the microtubule network revealed when cells are treated with Triton X-100. The inset shows a higher magnification of the cell nucleus. (B) Relative distribution of GFP-βII-tubulin in quantitative terms. The fluorescence intensity in similarly sized ROIs (red circles) was measured in the nucleus and the cytoplasm of the transfected cells. Numbers represent the calculated nuclear/cytoplasmic ratios in the cells shown. (C) Changes in nuclear/cytoplasmic ratios in the course of GFP-tubulin expression. Transiently transfected cells were cultured for 3-72 hours and the nuclear/cytoplasmic fluorescence intensity was determined for each time point in 90-200 specimens. Scale bars: 10 μm.

Table 1. Tubulin dynamics as determined by FRAP

Proteins	Localization	*n*	Mobile fraction (%)	$t_{1/2}$ (mobile) (seconds)	Range of $t_{1/2}$ (seconds)
βII-Tubulin	Nucleus	30	96.5±2.6	1.3±0.2	1.0-1.5
	Cytosol	30	95.6±3.9	2.2±0.8	1.2-3.4
βIV-Tubulin	Nucleus	30	95.3±4.4	1.3±0.3	1.0-2.0
	Cytosol	30	92.2±4.9	2.0±0.4	1.3-2.8
pEGFP-C1	Nucleus	15	98.3±2.2	0.6±0.2	0.4-0.8
	Cytosol				
ds-Red	Nucleus	16	97.1±3.1	0.6±0.2	0.4-0.8
	Cytosol				

74% of the cells that overexpressed disNES-1 showed nuclear/cytoplasmic ratios higher than 1.0. From these data, it can be safely concluded that nuclear export of β-tubulin is mediated primarily by NES-1.

Disruption of NES-1 induces cell cycle arrest at G0/G1

To explore the potential role of nuclear tubulin, we investigated the effect of GFP-βII-tubulin and GFP NES-disrupted βII-tubulin mutants on cell proliferation. For these purposes, we first determined the partitioning of transfected cells in the different phases of the cell cycle. As shown in Fig. 4D, although a shift from G2-M to G0-G1 sub-population could be observed in a small percentage of cells overexpressing wild-type and disNES-2-βII tubulin, the vast majority of HeLa cells overexpressing these tubulin forms, or GFP alone, were cycling normally 24 hours post-transfection. However, cells overexpressing disNES-1 were clearly arrested in the G0-G1 phase, as indicated by the drop in G2-M figures and the significant increase of pre-S cells (Fig. 4D). Assessment of DAPI staining intensity in cells transfected with wild type or disNES-1 and in surrounding unperturbed cells showed no changes in chromatin state (supplementary material Fig. S1), indicating that G0-G1 arrest is not due to global chromatin condensation and a subsequent transcriptional block. Partitioning of cells in the different phases of the cell cycle did not change significantly after 24 hours (not shown), but the number of cells overexpressing disNES-1 dropped precipitously after 72 hours in culture (8% and 63% of cells overexpressing disNES-1 and wild-type βII-tubulin, respectively). These results indicate that nuclear accumulation of βII-tubulin results in cell cycle arrest and could have detrimental consequences for cell survival.

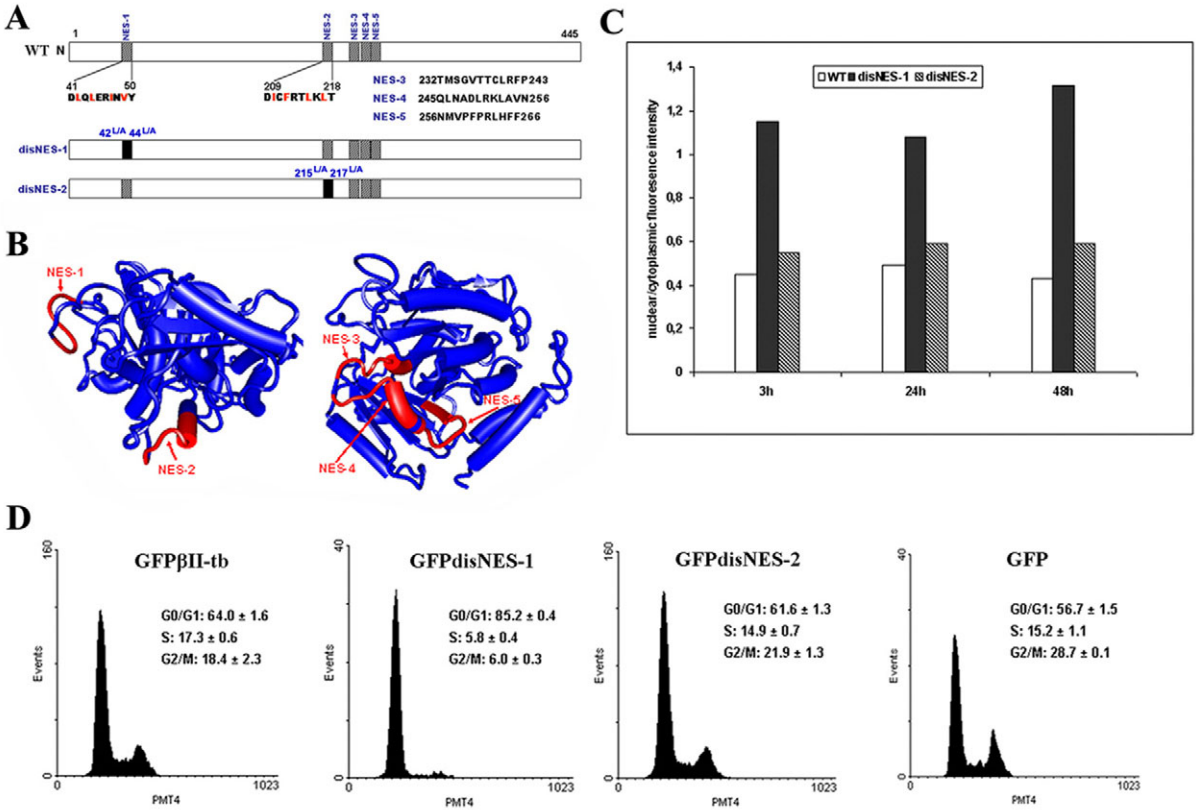

Fig. 4. Nuclear export of GFF β-tubulin is mediated by NES motifs. (A) Schematic representation of putative nuclear export sequences (NES) in wild-type (WT) human β-tubulin and two β-tubulin mutants with disrupted NES (disNES-1 and disNES-2). Two Leu residues in each NES sequences were replaced by Ala, as indicated. Hydrophobic amino acids in each NES are shown in red. (B) Schematic diagram of β-tubulin structure using 3D molecule viewer of the Vector NTI Suite software. The segments accommodating the putative NES are shown in red. (C) Histograms showing the ratio of nuclear/cytoplasmic fluorescence intensity in cells expressing wild-type and NES mutated GFP-tagged βII-tubulin. Between 110 and 200 cells were scored per treatment. (D) Cell cycle analysis of cells expressing GFP, wild-type (*GFPβII-tb*), NES-1 (*GFPdisNES-1*) and NES-2 (*GFPdisNES-2*) mutated β-tubulin. Percentages of viable cells in the G0-G1, S and G2-M phase are provided. Values are mean ± s.e.m. of measurements in three separate experiments.

Tubulin interacts specifically with histone H3

Seeking a rational basis that could explain the cell cycle-arresting effects described above, we investigated the potential interactions of soluble tubulin with nuclear proteins using a blot overlay assay. When a total cell extract was probed with purified brain tubulin under stringent conditions (1 M salt), a single band could be detected in the ligand blot. This protein had an electrophoretic profile resembling that of the core histones (Fig. 5A). To confirm that tubulin interacted with a specific histone subtype, we assayed binding to native histones purified from turkey erythrocytes. Tubulin bound exclusively to histone H3, despite the presence of the other histones and the much higher quantities of BSA and GST that were included as negative controls in the same reaction (Fig. 5A). Moreover, tubulin bound efficiently to recombinant (non-modified) histone H3, as well as to hyper-phosphorylated and hyper-acetylated histones H3 from HeLa cells (Fig. 5B), suggesting that this interaction is not affected by post-translational modifications and additional negative charge. The specificity of this in vitro association was further investigated using equal quantities of immobilized recombinant histones H3/H4 and various concentrations of tubulin. As shown in Fig. 5C, binding of tubulin to H3 was saturable and dose dependent.

The association of tubulin with H3 in vivo was examined by immunoprecipitation. Using extracts from HeLa cells treated with nocodazole in the cold (to induce nuclear accumulation of tubulin as shown in Fig. 1A), we found that tubulin specifically co-precipitates with histone H3 (Fig. 5D). These results suggested that the interactions detected could be relevant to the nuclear localization and retention of soluble tubulin.

Soluble tubulin could prevent the histone-mediated association of HP1 with LBR

We have previously reported that histones H3 and H4 'cross-link' heterochromatin protein 1 (HP1) and lamin B receptor (LBR) forming a tight, ternary complex (Polioudaki et al., 2001). To find out whether soluble tubulin affects the formation of this complex, we co-incubated GST-tagged HP1β and NtLBR (a water-soluble, N-terminal fragment that represents the entire nucleoplasmic domain of LBR) with recombinant H3, in the presence and absence of various amounts of purified brain tubulin. As shown in Fig. 6A, recombinant H3 bound to HP1β, but this association was almost completely inhibited when H3 and HP1 were co-incubated with tubulin. The same occurred with the two other HP1 variants (α and γ) when this assay was repeated (data not shown). Although tubulin did not bind directly to either GST or HP1 proteins (Fig. 6B), a small amount of this protein, probably associated with H3, was co-precipitated with the complex (Fig. 6A). Finally, tubulin inhibited the association of recombinant histone H3 with NtLBR in a dose-dependent fashion (Fig. 6C).

To examine the effect of tubulin on the formation of the HP1-H3/H4-LBR complex, we used GST-tagged NtLBR, His-tagged-HP1β and purified histones H3/H4. By means of pull-down assays, we could then show that H3/H4 bind to immobilized NtLBR, and that this sub-assembly associates with His-HP1β to form a quaternary complex. Incubation of the NtLBR-H3/H4 sub-complex with tubulin, prior addition of His-HP1β to the incubation mixture, prevented the association of His-HP1β with the sub-complex (Fig. 6D). Thus, tubulin seems to inhibit binding of H3 to HP1 and LBR, not allowing the formation of the corresponding multi-component assembly.

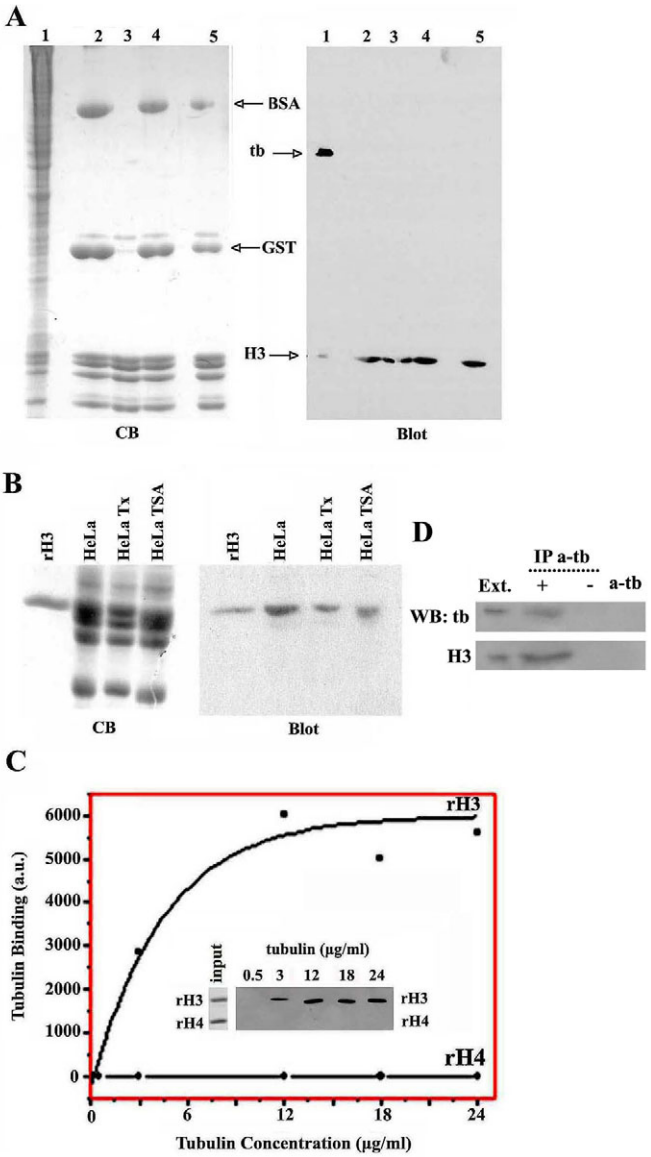

Fig. 5. Tubulin binding to histone H3. (A) Blot overlay assay using as a substrate a total cell extract (lanes 1), histone fractions isolated from turkey erythrocytes (lanes 3), and a mixture of histones and BSA and GST used as negative controls (lanes 2, 4 and 5). An SDS-PAGE profile after Coomassie Blue staining (CB) and a blot (Blot) probed with brain tubulin and developed by anti-β-tubulin antibodies are shown. (B) A similar assay with recombinant H3 (rH3) and histones from non treated cells (HeLa); cells treated with taxol (HeLa Tx) and cells treated with TSA (HeLa TSA). An SDS-PAGE profile after Coommasie Blue staining and a blot probed with brain tubulin and developed by anti-β-tubulin antibodies are shown. (C) Blot overlay assays using a fixed amount (input) of recombinant H3 and H4 as substrates and increasing quantities of brain tubulin as a probe. Bound tubulin was quantified by PC-based image analysis. (D) Co-precipitation of tubulin with histone H3. Immunoprecipitation (IP) of tubulin from HeLa extracts (Ext.) in the presence (+) or absence (–) of anti α-tubulin antibodies (a-tb). The samples were run on SDS-polyacrylamide gels and probed with anti α-tubulin (tb) and anti H3 (H3) antibodies (WB). For details on assays, see Materials and Methods.

Discussion

Prompted by the fact that many cytoplasmic and focal adhesion proteins are frequently found in the cell nucleus, we have investigated the subcellular distribution and dynamics of soluble tubulin. Results presented here reveal that (at least βII/IV) tubulin

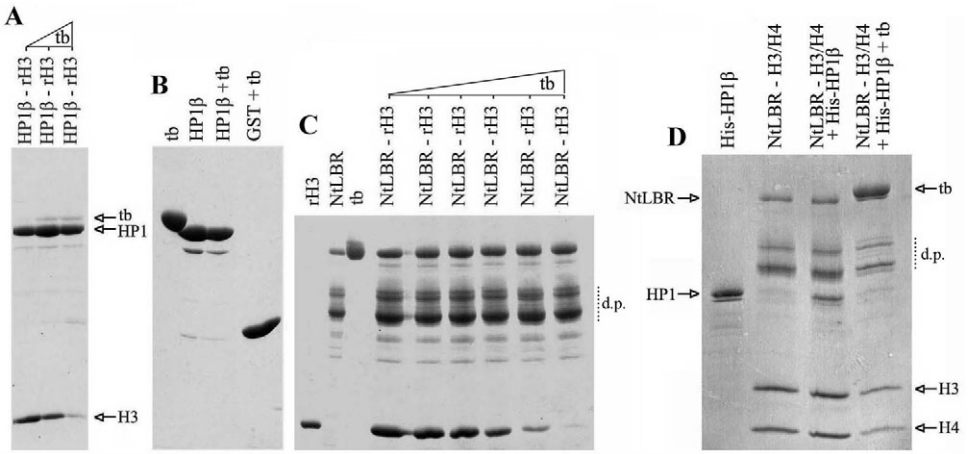

Fig. 6. Effect of tubulin on LBR-histone-HP1 complex formation. All panels show SDS-PAGE Coomassie Blue profiles from pull-down assays. (A) Recombinant H3 (rH3) precipitated by HP1β-GST (HP1β) in the presence of increasing amounts (triangle) of purified tubulin (tb). (B) Tubulin precipitated by HP1β-GST or a GST control (GST). (C) Precipitation of H3 after incubation of NtLBR-GST beads with a fixed amount of recombinant H3 and increasing amounts (triangle) of purified tubulin (tb). 'd.p.' shows the characteristic proteolytic products of recombinant NtLBR-GST that are produced after expression in bacteria. (D) NtLBR-GST was immobilized on glutathione beads and reacted sequentially with standard amounts of histones H3/H4 (*NtLBR-H3/H4*) and His-HP1β (*NtLBR-H3/H4+HisHP1β*), or histones H3/H4 (*NtLBR-H3/H4*), tubulin and His-HP1β (*NtLBR-H3/H4+HisHP1β+tb*). For details on assays, see Materials and Methods.

shuttles in and out the nucleus using an unusual method of nucleo-cytoplasmic transport: passage through the straits of the nuclear pore complex is accomplished by passive diffusion, whereas exit from the nucleus proceeds via a constitutive export system. β-Tubulin possesses at least one functional NES (NES-1) that seems to be recognized by exportin 1. When this signal is disrupted, soluble subunits accumulate in the nucleus and cell cycle progression is inhibited. This cell cycle arresting effect clearly suggests that nuclear accumulation of β-tubulin, which does not occur under normal circumstances, is a process of pathophysiological significance and may represent a defense mechanism against stress or malignant transformation. In that respect, it is interesting to note that GFP-tagged α-tubulin accumulates reversibly in nuclei of cultured tobacco cells, in response to low temperature (Schwarzerova et al., 2006), whereas nuclear β- and γ-tubulin have been so far detected primarily in cancer or transformed cells (Lesca et al., 2005; Walss-Bass et al., 2002; Xu and Luduena, 2002; Yeh and Luduena, 2004; Yeh et al., 2004).

Our findings echo results previously reported for other cytoplasmic and cytoskeletal proteins, such as the NAD+-dependent deacetylase SIRT2 [which, interestingly enough, acts on tubulin (see North and Verdin, 2007) and on actin (Wada et al., 1998)], that shuttle between the nucleus and the cytoplasm. Actin has been detected in the nucleus of HeLa cells upon stable transfection with GFP-β-actin, or microinjection with rhodamine conjugated β-actin (McDonald et al., 2006) and has been shown to accumulate in this compartment under various stressful or pathological conditions [e.g. treatment with DMSO, heat shock, ATP depletion, cellular senescence and intra-nuclear rod myopathy (Vartiainen, 2008)]. As in the case of soluble tubulin, the subcellular distribution of monomeric actin is regulated by constitutive nuclear export and involves two Leu-rich-type NESs. Disruption of these motifs results in nuclear accumulation and decreases significantly the proliferative potential of the cells (Wada et al., 1998).

The passive diffusion of α/β-tubulin, a complex of 110 kDa, through the nuclear pore complex can be explained by 'dilation' of the pore gate. It has been previously reported that the functional size of the central channel is variable and depends on the physiological state of the cells. Thus, the upper limit for nuclear import in normal proliferating BALB/c 3T3 cells is ~250 Å, whereas in quiescent populations, this value is decreased by some 100 Å (Feldherr and Akin, 1991) or increased about 40 Å (Feldherr et al., 1992). Changes of this magnitude could alter significantly the transport rates of large mRNP particles, ribosomal subunits or cytoplasmic proteins.

Our results suggest that chromatin is a potential target of nuclear tubulin. As tubulin has been found to interact with HALR/ALR and ASC-2 in the ASCOM complex (Goo et al., 2003), it is very likely that recruitment of ASCOM to target DNA response elements could be facilitated, or reinforced, by the strong binding of tubulin to histone H3. Tubulin-histone H3 interactions may also affect nuclear organization in a more direct way. A significant proportion of heterochromatin is localized at the periphery of the cell nucleus and maintains a close spatial association with the inner nuclear membrane (Bridger and Bickmore, 1998; Carvalho et al., 2001). This spatial association reflects a multiplicity of interactions between chromatin proteins (e.g. heterochromatin protein 1-HP1, BAF) and elements of the nuclear envelope (Georgatos, 2001). Under in vitro conditions, HP1 forms a tight complex with the inner nuclear membrane protein LBR and two of the core histones, H3 and H4 (Polioudaki et al., 2001). Moreover, all three variants of this protein (α, β, γ) target the nuclear periphery when injected into living cells and bind to isolated nuclear envelope/peripheral heterochromatin (NEPH) fractions isolated from turkey erythrocytes (Kourmouli et al., 2000). This association is potently inhibited by soluble tubulin (Kourmouli et al., 2001), which, as shown here, inhibits binding of histone H3 to HP1 and LBR, and prevents the formation of the HP1-histone-LBR complex. In this capacity, soluble tubulin may therefore represent an important 'switch' that regulates nuclear envelope-chromatin interactions during the cell cycle.

Accumulation of soluble tubulin in the nucleus does not cause a visible global change in chromatin condensation (this study). Therefore, potential changes in the gene expression program

resulting from 'uncoupling' of peripheral heterochromatin from attachment sites arranged at the inner nuclear membrane should be mechanistically distinct from those resulting from chromatin remodeling and unfolding. Clearly, more work is needed to understand whether disruption of the LBR-HP1-histone complex affects the transcriptional machinery, especially in loci that exhibit a peripheral nuclear localization and are positioned either near the nuclear lamina or at the gates of the nuclear pore complex.

Materials and Methods

Cell culture and treatments

The cervical adenocarcinoma cell line (HeLa) was obtained from the American Type Tissue Culture Collection (Manassas, VA) and maintained at 37°C in a humidified atmosphere containing 5% CO_2. HeLa cells were cultured in Dulbecco's MEM (Biochrom, Berlin, Germany), supplemented with 10% heat-inactivated fetal bovine serum, penicillin and streptomycin. To depolymerize microtubules, the cells were incubated at 4°C for 4 hours in the presence of nocodazole (33 μM for the first hour and 0.33 μM for the next three hours). To study the effect of leptomycin B (LMB) on the subcellular localization of endogenous tubulin, cells that had been pre-treated in the cold with nocodazole as described above were incubated for another 24 hours at 37°C in culture medium supplemented with 0.33 μM nocodazole, with and without 10 nM LMB.

Plasmid constructions and transient transfections

cDNA clones encoding HB9 (class βII-) and HB2 (class βIV-) human tubulin were obtained from RZPD (Accession Numbers BC055441 and BC019829, respectively). Plasmids expressing wild-type human βII- and βIV-tubulin fused with the Enhanced Green Fluorescent Protein at their N terminus were constructed by PCR amplification using 5′ and 3′ primers specifically designed to allow the cloning of the amplified fragments into the mammalian expression vector pEGFP-C1 (Clontech) through the *Eco*RI and *Sac*II sites. β-II-tubulin mutants disNES-1 and disNES-2 were constructed by overlap extension PCR (Ho et al., 1989). The sequences of all primers used in the PCR amplifications are shown in supplementary material Table S1. All mutant βII-tubulin cDNAs were sequenced for verification and found to contain the proper mutation. Transient transfections were performed using the calcium phosphate co-precipitation method. HeLa cells were plated in 6-well plates at a density of 10^5 cells/well the day before transfection and each well received a total of 3 μg of plasmid DNA.

FRAP

Fluorescence recovery after photobleaching (FRAP) assays were performed in a Leica laser scanning confocal microscope using suitable software and the 488 nm line of an Argon laser. Transfected cells were grown on special Petri dishes with coverslips attached and visualized in phenol-free culture medium buffered with HEPES-KOH. FRAP was performed employing a 1 μm spot bleach (either in the cytoplasm or in an area of the nucleoplasm exhibiting diffuse fluorescence) with a triple-bleach pulse of 208 mseconds. Bleaching was activated after taking 50 prebleach images. Five-hundred to 1000 images (256 by 256 pixels) were collected at a rate of 5 frames/second at low laser power (1.5-5.0% of the maximum value). Fluorescence recovery was monitored for until plateau was reached (several minutes in some cases). For normalizing the data, we always corrected for fluorescence quench and recovery observed in the entire cell and in the background.

Immunofluorescence and confocal microscopy

Indirect immunofluorescence was performed as described previously (Theodoropoulos et al., 1999). Briefly, cells grown on coverslips were washed with PBS, fixed in 4% formaldehyde for 10 minutes at room temperature and permeabilized with Triton X-100. Fixed cells were incubated in blocking buffer [phosphate-buffered saline (pH 7.4), 0.5% Triton X-100 and 1% fish skin gelatin] and stained with primary and secondary antibodies for 45 minutes. The primary antibodies used included anti-α- and anti-β tubulin monoclonal antibodies, obtained from Sigma (St Louis, MO) and an anti-lamin B polyclonal antibody (Simos and Georgatos, 1992). Several secondary antibodies were used, including anti-rabbit and anti-mouse immunoglobulins conjugated to FITC or Alexa 555. Chromatin was decorated by the DNA-binding dye Topro.

Quantification of fluorescence intensity

To evaluate nuclear accumulation of GFP-tagged tubulin isoforms, we measured the fluorescence intensity of selected circular areas incorporating 200 pixels in both the nucleus and the cytoplasm of each cell, using a purposely developed MATLAB (The Mathworks, MA, USA) script. Results were expressed as ratios of nuclear/cytoplasmic fluorescence intensity.

Cell cycle analysis

Cells were trypsinized, washed with PBS and fixed consecutively with 1% formaldehyde for 1 hour at 4°C and 70% ethanol (in PBS) for an additional hour at 4°C. For DNA staining, fixed cells were resuspended in PBS containing ribonuclease A and propidium iodide (PI) at final concentration of 100 and 40 μg/ml, respectively, and incubated at 37°C for 30 minutes in the dark. Experiments were performed in triplicate and samples were analyzed by flow cytometry using an Epics Elite flow cytometer (Coulter, Miami, FL). Cell cycle analysis of GFP stained cells was carried out using WinMDI software (Windows Multiple Document Interface for Flow Cytometry).

Preparation of proteins

Tubulin was obtained from a 100,000 ***g*** pig brain supernatant by two cycles of assembly-disassembly and further purified by phosphocellulose chromatography (P11, Whatman) in column buffer [25 mM PIPES (pH 6.9), 1 mM EGTA, 0.5 mM $MgSO_4$] containing 1 mM Mg-GTP, 1 mM DTT and protease inhibitors. Native histones were extracted from turkey erythrocyte nuclei, isolated as specified previously (Georgatos and Blobel, 1987), with 0.2 M H_2SO_4, and precipitated with eight volumes of cold acetone. Histone pellets were dissolved in distilled water and stored at –80°C. Histones H3 and H4 were isolated from turkey erythrocyte nuclei by ion-exchange chromatography. Alternatively, hyperphosphorylated and hyperacetylated histones were isolated from cultured cells. To this end, HeLa cells were treated either with 100 μM Taxol (Bristol-Meyer Squibb Company) or 1 mg/ml trichostatin A (TSA) for 20 hours, to induce mitotic phosphorylation and hyperacetylation, respectively. Glutathione S-transferase (GST), fused proteins, His_6-tagged HP1β and recombinant histones H3 and H4 were expressed in BL21 (DE3) cells and purified from lysates according to standard procedures.

Blot overlay assays

Proteins were separated by SDS-PAGE, transferred to nitrocellulose membranes and incubated overnight at 4°C with blocking buffer [20 mM Tris-HCl (pH 7.4), 155 mM NaCl, 0.1% Tween-20, 1% gelatin]. Then, the membranes were incubated with the 'probe' (tubulin; 3 μg/ml in a typical assay) in overlay buffer [20 mM Tris-HCl (pH 7.4), 600 mM NaCl, 0.1% Tween-20, 1% gelatin) at room temperature for 1 hour and washed five times with the same buffer. After incubation with anti β-tubulin (clone TUB2.1, Sigma) antibodies, blots were washed five times and processed for ECL. Band intensities were quantified by PC-based Image Analysis (Image Analysis, Ontario, Canada).

Pull-down assays

GST fusion proteins (NtLBR-GST, HP1α-GST, HP1β-GST, HP1γ-GST or GST alone; 30 μg) were incubated for 30 minutes at room temperature with 30 μl of glutathione-sepharose 4B beads (GE Healthcare Bio-Sciences, Piscataway, NJ) in 150 mM NaCl buffer ST [20 mM Tris-HCl (pH 7.5), 250 mM sucrose, 2 mM $MgCl_2$, 0.1 mM EGTA, 1 mM DTT, 1 mM PMSF, protease inhibitors, 1% Triton X-100]. After washing three times with the same medium, the beads were combined with different proteins and further incubated for 1 hour at room temperature. In the experiments shown in Fig. 6, HP1-GST beads were incubated in 150 μl 500 mM NaCl ST buffer with 15 μg of recombinant H3 in the absence or presence of 5 μg and 15 μg purified tubulin (Fig. 6A). In control experiments, HP1-GST and GST beads were incubated in 150 μl 500 mM NaCl ST buffer with 15 μg of purified tubulin (Fig. 6B). NtLBR-GST beads were combined in 200 μl 300 mM NaCl ST buffer with either 15 μg of recombinant H3 in the absence or the presence of 5, 15, 30, 50 and 100 μg of purified tubulin (Fig. 6C) or 30 μg of purified turkey H3/H4 (Fig. 6D). The complex NtLBR-H3/H4 was then incubated in 500 μl 300 mM NaCl ST buffer with 45 μg His-HP1β or 150 μg tubulin, and 45 μg His-HP1β was added sequentially (Fig. 6D). The beads were washed five times with buffer ST before eluting the bound proteins with hot Laemmli buffer.

Immunoprecipitation and immunoblotting

HeLa cells grown on Petri dishes were incubated at 4°C for 4 hours in the presence of nocodazole (33 μM for the first hour and 0.33 μM for the next 3 hours) to depolymerize microtubules and induce nuclear accumulation of α,β-tubulin (see Fig. 1). Cells were extracted with lysis buffer [50 mM HEPES (pH 7.5), 140 mM NaCl, 0.1% deoxycholate, 1% Triton X-100, 0.5 mM PMSF and protease inhibitors] for 10 minutes on ice. After sonication, the supernatant was clarified (12,000 ***g***, 10 minutes, 4°C), pre-absorbed on G-sepharose beads (GE Healthcare Bio-Sciences) and incubated with or without anti α-tubulin monoclonal antibodies (Sigma Chemical Co), overnight at 4°C. The immune complexes were incubated with G-sepharose beads for 1.5 hours at 4°C, recovered by centrifugation (3000 ***g***, 2 minutes, 4°C), washed seven times with lysis buffer and solubilized in TrueBlot ULTRA (eBioscience, San Diego, CA) hot sample buffer. Samples were electrophoresed on SDS-polyacrylamide gels and transferred on nitrocellulose membranes. Then, they were immunoblotted with mouse anti α-tubulin (Sigma Chemical Co., 1:500) or goat anti H3 (Santa Cruz, CA, 1:300) primary antibodies and incubated with horseradish peroxidase-conjugated anti-mouse (GE Healthcare Bio-Sciences, 1:10,000) or anti-goat (Sigma, 1:1000), respectively. Because tubulin and heavy chains of IgG have the same electrophoretic mobility, we performed immunoblotting using TrueBlotTM

ULTRA (eBioscience) as specified by the supplier. This procedure enabled detection of tubulin, without hindrance, by interfering immunoprecipitating Ig heavy and light chains. Signals were visualized by enhanced chemiluminescence (ECL kit, GE Healthcare Bio-Sciences).

This work was supported partly from the Greek Secretariat of Research and Technology (PENED 01EΔ376) and the Cretan Association for Biomedical Research. The authors thank Prof. Elias Castanas, George Mavrothalassitis (University of Crete) and Anastasia Politou (University of Ioannina) for helpful discussions and advice, Dr Stefan Terjung (Advanced Light Microscopy Facility, EMBL) and Dr George Dialynas (University of Ioannina) for helping with FRAP experiments, Dr Harilaos Ginis (University of Crete) for helping with image processing, and Paraskevi Papakosta (University of Crete) for technical support.

References

Bridger, J. M. and Bickmore, W. A. (1998). Putting the genome on the map. *Trends Genet.* **14**, 403-409.

Burkhart, C. A., Kavallaris, M. and Band Horwitz, S. (2001). The role of beta-tubulin isotypes in resistance to antimitotic drugs. *Biochim. Biophys. Acta* **1471**, O1-O9.

Carvalho, C., Pereira, H. M., Ferreira, J., Pina, C., Mendonca, D., Rosa, A. C. and Carmo-Fonseca, M. (2001). Chromosomal G-dark bands determine the spatial organization of centromeric heterochromatin in the nucleus. *Mol. Biol. Cell* **12**, 3563-3572.

Feldherr, C. M. and Akin, D. (1991). Signal-mediated nuclear transport in proliferating and growth-arrested BALB/c 3T3 cells. *J. Cell Biol.* **115**, 933-939.

Feldherr, C. M., Lanford, R. E. and Akin, D. (1992). Signal-mediated nuclear transport in simian virus 40-transformed cells is regulated by large tumor antigen. *Proc. Natl. Acad. Sci. USA* **89**, 11002-11005.

Georgatos, S. D. (2001). The inner nuclear membrane: simple, or very complex? *EMBO J.* **20**, 2989-2994.

Georgatos, S. D. and Blobel, G. (1987). Two distinct attachment sites for vimentin along the plasma membrane and the nuclear envelope in avian erythrocytes: a basis for a vectorial assembly of intermediate filaments. *J. Cell Biol.* **105**, 105-115.

Goo, Y. H., Sohn, Y. C., Kim, D. H., Kim, S. W., Kang, M. J., Jung, D. J., Kwak, E., Barlev, N. A., Berger, S. L., Chow, V. T. et al. (2003). Activating signal cointegrator 2 belongs to a novel steady-state complex that contains a subset of trithorax group proteins. *Mol. Cell. Biol.* **23**, 140-149.

Gu, Y. and Ihara, Y. (2000). Evidence that collapsin response mediator protein-2 is involved in the dynamics of microtubules. *J. Biol. Chem.* **275**, 17917-17920.

Ho, S. N., Hunt, H. D., Horton, R. M., Pullen, J. K. and Pease, L. R. (1989). Site-directed mutagenesis by overlap extension using the polymerase chain reaction. *Gene* **77**, 51-59.

Kourmouli, N., Theodoropoulos, P. A., Dialynas, G., Bakou, A., Politou, A. S., Cowell, I. G., Singh, P. B. and Georgatos, S. D. (2000). Dynamic associations of heterochromatin protein 1 with the nuclear envelope. *EMBO J.* **19**, 6558-6568.

Kourmouli, N., Dialynas, G., Petraki, C., Pyrpasopoulou, A., Singh, P. B., Georgatos, S. D. and Theodoropoulos, P. A. (2001). Binding of heterochromatin protein 1 to the nuclear envelope is regulated by a soluble form of tubulin. *J. Biol. Chem.* **276**, 13007-13014.

Krajci, D., Mares, V., Lisa, V., Bottone, M. G. and Pellicciari, C. (2006). Intranuclear microtubules are hallmarks of an unusual form of cell death in cisplatin-treated C6 glioma cells. *Histochem. Cell Biol.* **125**, 183-191.

Lesca, C., Germanier, M., Raynaud-Messina, B., Pichereaux, C., Etievant, C., Emond, S., Burlet-Schiltz, O., Monsarrat, B., Wright, M. and Defais, M. (2005). DNA damage induce gamma-tubulin-RAD51 nuclear complexes in mammalian cells. *Oncogene* **24**, 5165-5172.

Lowe, J., Li, H., Downing, K. H. and Nogales, E. (2001). Refined structure of alpha beta-tubulin at 3.5 A resolution. *J. Mol. Biol.* **313**, 1045-1057.

Lu, Q. and Luduena, R. F. (1994). *In vitro* analysis of microtubule assembly of isotypically pure tubulin dimers. Intrinsic differences in the assembly properties of alpha beta II, alpha beta III, and alpha beta IV tubulin dimers in the absence of microtubule-associated proteins. *J. Biol. Chem.* **269**, 2041-2047.

Luduena, R. F. (1998). Multiple forms of tubulin: different gene products and covalent modifications. *Int. Rev. Cytol.* **178**, 207-275.

Martin, L., Fanarraga, M. L., Aloria, K. and Zabala, J. C. (2000). Tubulin folding cofactor D is a microtubule destabilizing protein. *FEBS Lett.* **470**, 93-95.

McDonald, D., Carrero, G., Andrin, C., de Vries, G. and Hendzel, M. J. (2006). Nucleoplasmic beta-actin exists in a dynamic equilibrium between low-mobility polymeric species and rapidly diffusing populations. *J. Cell Biol.* **172**, 541-552.

McKean, P. G., Vaughan, S. and Gull, K. (2001). The extended tubulin superfamily. *J. Cell Sci.* **114**, 2723-2733.

Menko, A. S. and Tan, K. B. (1980). Nuclear tubulin of tissue culture cells. *Biochim. Biophys. Acta* **629**, 359-370.

Mirski, S. E., Bielawski, J. C. and Cole, S. P. (2003). Identification of functional nuclear export sequences in human topoisomerase IIalpha and beta. *Biochem. Biophys. Res. Commun.* **306**, 905-911.

Mithieux, G., Alquier, C., Roux, B. and Rousset, B. (1984). Interaction of tubulin with chromatin proteins: H1 and core histones. *J. Biol. Chem.* **259**, 15523-15531.

Nogales, E., Wolf, S. G. and Downing, K. H. (1998). Structure of the alpha beta tubulin dimer by electron crystallography. *Nature* **391**, 199-203.

North, B. J. and Verdin, E. (2007). Interphase nucleo-cytoplasmic shuttling and localization of SIRT2 during mitosis. *PLoS ONE* **2**, e784.

Ovechkina, Y., Maddox, P., Oakley, C. E., Xiang, X., Osmani, S. A., Salmon, E. D. and Oakley, B. R. (2003). Spindle formation in Aspergillus is coupled to tubulin movement into the nucleus. *Mol. Biol. Cell* **14**, 2192-2200.

Polioudaki, H., Kourmouli, N., Drosou, V., Bakou, A., Theodoropoulos, P. A., Singh, P. B., Giannakouros, T. and Georgatos, S. D. (2001). Histones H3/H4 form a tight complex with the inner nuclear membrane protein LBR and heterochromatin protein 1. *EMBO Rep.* **2**, 920-925.

Rezania, V., Azarenko, O., Jordan, M. A., Bolterauer, H., Luduena, R. F., Huzil, J. T. and Tuszynski, J. A. (2008). Microtubule assembly of isotypically purified tubulin and its mixtures. *Biophys. J.* **95**, 1993-2008.

Schwarzerova, K., Petrasek, J., Panigrahi, K. C., Zelenkova, S., Opatrny, Z. and Nick, P. (2006). Intranuclear accumulation of plant tubulin in response to low temperature. *Protoplasma* **227**, 185-196.

Simos, G. and Georgatos, S. D. (1992). The inner nuclear membrane protein p58 associates *in vivo* with a p58 kinase and the nuclear lamins. *EMBO J.* **11**, 4027-4036.

Sullivan, K. F. (1988). Structure and utilization of tubulin isotypes. *Annu. Rev. Cell Biol.* **4**, 687-716.

Theodoropoulos, P. A., Polioudaki, H., Kostaki, O., Derdas, S. P., Georgoulias, V., Dargemont, C. and Georgatos, S. D. (1999). Taxol affects nuclear lamina and pore complex organization and inhibits import of karyophilic proteins into the cell nucleus. *Cancer Res.* **59**, 4625-4633.

Vartiainen, M. K. (2008). Nuclear actin dynamics: from form to function. *FEBS Lett.* **582**, 2033-2040.

Wada, A., Fukuda, M., Mishima, M. and Nishida, E. (1998). Nuclear export of actin: a novel mechanism regulating the subcellular localization of a major cytoskeletal protein. *EMBO J.* **17**, 1635-1641.

Walss-Bass, C., Xu, K., David, S., Fellous, A. and Luduena, R. F. (2002). Occurrence of nuclear beta(II)-tubulin in cultured cells. *Cell Tissue Res.* **308**, 215-223.

Xu, K. and Luduena, R. F. (2002). Characterization of nuclear betaII-tubulin in tumor cells: a possible novel target for taxol. *Cell Motil. Cytoskeleton* **53**, 39-52.

Yanagida, M., Hayano, T., Yamauchi, Y., Shinkawa, T., Natsume, T., Isobe, T. and Takahashi, N. (2004). Human fibrillarin forms a sub-complex with splicing factor 2-associated p32, protein arginine methyltransferases, and tubulins alpha 3 and beta 1 that is independent of its association with preribosomal ribonucleoprotein complexes. *J. Biol. Chem.* **279**, 1607-1614.

Yeh, I. T. and Luduena, R. F. (2004). The betaII isotype of tubulin is present in the cell nuclei of a variety of cancers. *Cell Motil. Cytoskeleton* **57**, 96-106.

Yeh, T. S., Hsieh, R. H., Shen, S. C., Wang, S. H., Tseng, M. J., Shih, C. M. and Lin, J. J. (2004). Nuclear betaII-tubulin associates with the activated notch receptor to modulate notch signaling. *Cancer Res.* **64**, 8334-8340.